# Tunable metallo-hydrogels: Mechanical properties and characterization of stimuli responsive self-assembling peptide hydrogels

Alexia Tialiou[1,2], Christopher J. Serpell[3], Lingcong Ge[1,2], Jia Min Chin*[4], Bernhard K. Keppler[1,5], Michael R. Reithofer*[1]

[1]Institute of Inorganic Chemistry, Faculty of Chemistry, University of Vienna, Währinger Str. 42, 1090 Vienna, Austria. Email: michael.reithofer@univie.ac.at

[2]Vienna Doctoral School in Chemistry (DoSChem), University of Vienna, Währinger Str. 42, 1090 Vienna, Austria.

[3]School of Pharmacy, University College London, 29/39 Brunswick square, London, WC1N1AX, United Kingdom.

[4]Institute of Functional Materials and Catalysis, Faculty of Chemistry, University of Vienna, Währinger Str. 42, 1090 Vienna, Austria. Email: jiamin.chin@univie.ac.at

[5]University of Vienna and Medical University of Vienna, Research Cluster "Translational Cancer Therapy Research", Währinger Str. 42, 1090 Vienna, Austria.

## Abstract

Supramolecular self-assembly is employed in this study to design short amphiphilic peptides with specific binding affinity for Zn(II). Two selectively modified peptides (Ac-LIVKHH-$NH_2$, P1 & Fmoc-LIVKHH-$NH_2$, P2) were synthesized using standard Fmoc-/Boc- solid-phase peptide synthesis. When these water-soluble peptides are combined with Zn(II) salt solution, they encapsulate large volumes of water to form metallo-hydrogels. The Zn(II) responsiveness in metallo-hydrogels was investigated in buffer or water (pH 7) with or without Zn(II) salts. The afforded supramolecular architectures (metallo-hydrogels) were characterized by circular dichroism and their micro- and nanostructure with scanning electron microscopy (SEM) and transmission electron microscopy (TEM), respectively. Measurements of rheology and thixotropy were conducted to assess the gelation behavior, the viscoelastic character and the mechanical properties of metallo-hydrogels. We found that Zn(II) significantly influences hydrogel formation, leading to improved mechanical properties. The resulting hydrogels show remarkable thixotropic behavior, indicating their potential in 3D printing and as injectable carriers. Such hydrogels can be also used as primary wound dressings, and their antibacterial activity can be further explored. This research work provides valuable insights into the zinc-responsive behavior of the aforementioned peptides, establishing a foundation for their prospective applications in biomaterials and materials science.

Keywords: peptide hydrogels; self-assembly; amphiphilic peptides; zinc; metallo-hydrogels; thixotropy

## 1. Introduction

Molecular self-assembly refers to the spontaneous and reversible organization of molecules into higher-order structures.[1, 2] This phenomenon is highly prevalent in nature, where assembled entities such as DNA or proteins exhibit distinctive biological functions.[3] Peptide-based supramolecular architectures stand out for their biocompatibility, biodegradability, and ease of synthesis.[4, 5] Such structures are based on the organization of peptides into secondary structures such as β-sheet or α-helix, which can then undergo hierarchical and multiscale assembly processes.[6-8] These structures rely on non-covalent interactions, such as hydrogen bonds, hydrophobic interactions, van der Waals forces, electrostatic- and π-π interactions, respectively.[9]

In aqueous solution, these self-assembled peptide architectures can also yield hydrogels by entrapping large amounts of water.[10-12] To generate peptide hydrogels, the use of short peptides is particularly appealing as it offers robustness, scalability, and cost-effectiveness.[4, 7, 13-15] Besides the rational design of short peptides, a common strategy to modulate the self-assembling properties involves protection of the *N*- and/or *C*-terminus through use of acetyl or large aromatic groups such as fluorenylmethoxycarbonyl protecting group (Fmoc).[14, 16-18] This modification reduces charge repulsions and introduces π-stacking/hydrophobic contributions, thereby promoting self-assembly and hydrogel formation.[19-21]

Metal ions are frequently employed to trigger peptide assembly, thereby leading to hydrogelation.[22-25] Such metal ion-coordinated peptide hydrogels hold significant potential, as they exploit the unique physicochemical characteristics of metals, such as Zn(II), which play essential roles in biological processes and disease-related protein assemblies.[13, 26-29] For instance, zinc, known for its antimicrobial and bacteriostatic properties, is beneficial in wound healing and infection prevention applications.[22, 30-34] Additionally, zinc plays a crucial role in collagen synthesis, imparting tensile strength to the newly formed tissue at the wound site.[35] However, a comprehensive understanding of the impact of metal coordination on peptide assembly processes affording hydrogels remains limited. The addition of metal ions through metal-ligand coordination offers a method to tune the mechanical stiffness of hydrogels, complementing the other approaches of

https://doi.org/10.26434/chemrxiv-2024-00pc3 **ORCID:** https://orcid.org/0000-0002-6328-1896 Content not peer-reviewed by ChemRxiv. **License:** CC BY 4.0

manipulating crosslink density, peptide concentration, or pH, which can influence the essential biological functions of such gels.[23, 36-39] Metal salts or complexes have been utilized to induce gelation in peptide solutions, enabling formation of stable gels through ordered aggregates formed by metal-peptide interactions.[11, 24, 28, 36, 37, 39] For example, Mishra and coworkers investigated the influence of metal salts on the self-assembling behavior of Ac-LIVAGD and Ac-IVD, revealing how cation coordination and ionic strength affect hydrogelation, facilitating controlled modulation of the mechanical properties of Ac-LIVAGD hydrogel for targeted biomedical applications.[40]

Herein, short amphiphilic peptides were developed with specific binding affinity for biologically benign metal salts, particularly zinc. In aqueous conditions, the interactions between the histidine moieties of peptides and Zn(II) resulted in the formation of a coordination polymer incorporating zinc as a crosslinker, ultimately leading to metallo-hydrogel formation. We investigated the impact of *N*-terminus modifications on hydrogel formation, whereby Fmoc-protected peptides were found to yield stiffer hydrogels due to favorable π-π stacking effects. This comprehensive analysis demonstrates the zinc-responsive behavior of the metallo-hydrogels, covering variations in zinc content ranging from 0 to 0.5 equivalents. The influence of Zn(II) on their mechanical properties, viscoelastic character, and recovery capabilities was also assessed. The observed effects demonstrate how zinc plays a key role in enhancing the overall performance of the metallo-hydrogels, providing valuable insights into their potential applications in the field of materials science and biomaterials.

## 2. Materials and methods

### 2.1 Materials for peptide synthesis

Fmoc rink amide AM resin (resin 0.78 mmol $g^{-1}$) was purchased from Merck. The series of Fmoc protected amino acids including leucine, isoleucine, valine, lysine, and histidine, as well as diisopropylethylamine (DIPEA) were purchased from Iris Biotech; (2-(1H-benzotriazol-1-yl)-1,1,3,3-tetramethyluronium hexafluorophosphate (HBTU) from Acros-Fischer; trifluoroacetic acid (peptide grade, TFA) from Fluorochem Limited; triisopropylsilane (TIS) from TCI Europe; piperidine (99%) from Alfa Aesar; diethyl ether ($Et_2O$) and dichloromethane (DCM) from ChemSolute; dimethylformamide (DMF) from Fischer Chemical, and acetic anhydride ($Ac_2O$) from Sigma Aldrich. Kaiser test reagents were prepared according to literature, potassium cyanide and pyridine were acquired from Merck and Acros-Fischer, respectively (reagent A), n-butanol and ninhydrin from Alfa Aesar (reagent B), and phenol and n-butanol from Alfa Aesar and Acros-Fischer, respectively, (reagent C).[41] For gel preparation, PBS (phosphate-buffered saline 10x) was used as purchased from Alfa Aesar and MES (2-(*N*-morpholino)ethanesulfonic acid), purchased from BLD Pharmatech Ltd, was prepared according to an online protocol.[42] Collagen Type I was purchased from MP Biomedicals, USA. Milli-Q reagent water (18.2 MΩ cm, 25 °C, Millipore, UK) was used for all experiments.

### 2.2 Peptide synthesis and purification

Ac-LIVKHH-$NH_2$ (**P1**) and Fmoc-LIVKHH-$NH_2$ (**P2**) peptides were synthesized based on Fmoc/Boc solid phase peptide chemistry.[43, 44] In brief, Fmoc-rink amide AM resin (0.78 mmol $g^{-1}$) was weighed out, and the beads were allowed to swell for 1h in DMF. Fmoc deprotection was achieved with a mixture of 20% v/v piperidine in DMF, which was added to the resin and left to agitate for 15 min. After thorough washing with DMF, 2 equiv. of HOBt and HBTU were dissolved in DMF and combined. Another 2 equiv. of the initial protected amino acid, pre-dissolved in DMF, were introduced to the mixture, followed by the addition of 2 equiv. of DIPEA to the same solution, allowing 20 seconds for activation. Subsequently, this solution was added to the resin and left to agitate for 45 minutes. The resin was washed with DMF and subjected to a series of deprotection and coupling reactions with the desired amino acids. All the reactions were performed at 25°C, and the couplings were monitored via Kaiser test. After a though washing with DMF, a DMF solution of 12 equiv. of $Ac_2O$ and DIPEA was added (capping) to prevent side reactions of the side-groups, and the mixture was incubated for 30 minutes. To obtain the **P1**, the Fmoc group of the final amino acid was deprotected. Then, the *N*-terminus of **P1** was acetylated using a 5-times excess of $Ac_2O$ and DIPEA. In case of **P2** the *N*-terminus remained intact with the Fmoc group still attached. The resin was subsequently washed with DMF and DCM and allowed to dry before the peptide cleavage step using a mixture of 94% TFA, 3% Milli-Q water and 3% TIS. The solvents were reduced under an argon atmosphere, and $Et_2O$ was added to precipitate the peptide. The peptides were isolated through several centrifugations, washed with $Et_2O$, and dried under reduced pressure. The peptides were then lyophilized in Milli-Q water with the presence of 0.01% TFA and analyzed by high-performance liquid chromatography system coupled to a mass spectrometer (HPLC-MS, Thermo scientific, Ultimate 3000 HPLC system coupled with maXis UHR-TOF). The purity of the desired peptides ranged between 95 and 99%, therefore, no further purification was necessary. ESI-MS spectra were measured on a Brucker maXis UHR-TOF equipped with ESI electrospray ionization chamber in positive mode. Yield: **P1**: 287 mg (57.4%); **P2**: 379 mg (75.8%), ESI-MS: Calculated for $C_{37}H_{62}N_{12}O_7$ (786.98, **P1**) and $C_{50}H_{70}N_{12}O_8$ (967.19, **P2**) ($[M+H^+]^+$), found m/z 787.52 (**P1**) and 967.55 (**P2**).

https://doi.org/10.26434/chemrxiv-2024-00pc3 **ORCID:** https://orcid.org/0000-0002-6328-1896 Content not peer-reviewed by ChemRxiv. **License:** CC BY 4.0

## 2.3 Nuclear magnetic resonance (NMR)

$^{1}$H and $^{13}$C-NMR spectra were recorded in $D_2O$ on a Brucker BioSpin AV NEO 600 MHz spectrometer. During sample preparation, 5 mg of peptide powder were dissolved in $D_2O$. Later, 600 µL of the solution was transferred into an NMR tube.

**P1** $^{1}$H-NMR (100% $D_2O$): δ = 8.56 (dd, 2H), 7.29 (dd, 2H), 4.65 (t, 2H), 4.28 (dd, 2H), 4.19 (d, 1H), 4.06 (d, 1H), 3.24 (m, 2H), 3.16 (m, 2H), 2.98 (t, 2H), 1.85 (m, 1H), 1.67 (m, 5H), 1.59 (m, 4H), 1.42 (m, 1H), 1.36 (m, 1H), 1.21 (m, 1H), 0.88 (m, 21H) ppm. $^{13}$C-NMR (100% $D_2O$): δ = 174.76, 174.13, 173.53, 173.32, 173.00, 171.23, 133.58, 133.47, 128.18, 128.09, 117.29, 117.23, 115.47, 59.32, 57.93, 53.19, 52.63, 52.42, 52.28, 39.67, 39.10, 35.63, 30.35, 29.99, 26.44, 26.39, 26.15, 24.46, 24.26, 22.12, 21.87, 21.45, 21.00, 18.25, 17.82, 14.64, 9.62 ppm.

**P2** $^{1}$H-NMR (100% $D_2O$): δ = 8.61 (d, 2H), 7.92 (d, 2H), 7.69 (dd, 2H), 7.50 (t, 2H), 7.43 (q, 2H), 7.29 (d, 2H), 4.64 (q, 3H), 4.54 (m, 1H), 4.32 (t, 1H), 4.25 (m, 1H), 4.10 (d, 1H), 4.00 (, 2H), 3.23 (td, 2H), 3.1 (, 2H), 2.95 (t, 2H), 1.48 (, 1H), 1.33 (m, 2H), 1.43 (m, 4H), 1.67 (m, 4H), 1.81 (m, 1H), 1.97 (m, 1H), 0.86 (d, 4H), 0.81 (s, 13H), 0.72 (d, 1H) ppm. $^{13}$C-NMR (100% $D_2O$): δ = 173.70, 173.49, 173.17, 171.35, 163.06, 157.72, 144.04, 143.63, 141.06, 133.69, 133.57, 128.30, 128.16, 127.6, 125.07, 125.00, 124.85, 120.24, 118.89, 117.25, 117.38, 117.32, 115.59, 113.94, 66.75, 59.47, 59.26, 58.25, 57.84, 53.73, 53.30, 52.53, 52.39, 47.36, 47.18, 39.93, 39.20, 35.65, 30.39, 30.21, 30.02, 26.50, 26.24, 24.64, 24.37, 24.20, 22.21, 22.11, 18.34, 17.91 ppm.

## 2.4 Hydrogel preparation

All hydrogels were prepared using either Milli-Q water (with the pH adjusted with 750 mM NaOH solution to approximately pH = 7), phosphate-buffered saline (PBS 10X, pH 7.4) or 2-(*N*-morpholino)ethanesulfonic acid buffer solution (MES, pH 6.4) at room temperature (25 °C). The 0.5 M MES buffer was prepared by dissolving MES in Milli-Q water and adjusting the pH with 10N NaOH solution. Briefly, pre-weighed peptide powder of **P1** and **P2** was dissolved in total volume of 1 or 2 mL (depending on the measurement) in Milli-Q water, and then 0.5 equiv. of $Zn(OAc)_2$ was added to the solution. The vial was vortexed and sonicated for 10-20 sec to achieve a homogenous solution. The pH was then adjusted to approximately 7 using 750 mM NaOH solution. Similarly, buffer-containing hydrogels were prepared using 10% buffer in Milli-Q water and then added 0.5 equiv. of $Zn(OAc)_2$. The glass vial, where hydrogels prepared, was vortexed for 10-20 sec to achieve an even distribution of the buffer. Similar hydrogels were prepared also in absence of $Zn(OAc)_2$. The vials were kept on the bench, and hydrogel formation was initially observed over time via the vial inversion method and later was verified through rheology (see section 3.3). Collagen hydrogels were prepared by dissolving collagen type I in MQ to a concentration of 0.8 wt% (7.5 mg $mL^{-1}$) for **P1** and 1 wt% (9.5 mg $mL^{-1}$) for **P2.** PBS was then added to achieve 10% PBS concentration in the final solution. The solution was titrated to pH 7.4 using 0.1 M of NaOH. Gelation occurred at 37°C in 1 h.[26]

## 2.5 Circular Dichroism (CD)

CD measurements were conducted on a Chirascan Plus (Applied Photophysics) spectrometer using a quartz cuvette with an optical path length of 0.01 mm. Peptide solutions with concentrations ranging from 2 to 50 mM, dissolved in Milli-Q water or MES buffer, were monitored at room temperature (25 °C) within a wavelength range of 190-280 nm in steps of 1 nm and with a spectral bandwidth of 1 nm. The spectra were acquired as an average of 5 runs for each sample. A baseline correction of all spectra was performed either in Milli-Q water of buffer, depending on the measurement. CD signals were further normalized to the molar ellipticity value.

## 2.6 Viscoelastic characterization of peptide hydrogels

Rheology measurements were performed using an HR-2 Discovery Hybrid Rheometer (TA Instruments) with 25 mm diameter aluminum plates using parallel geometry and connected with a Peltier plate to control the temperature, with a gap distance of 450 µm. The viscoelastic properties and mechanical stiffness of the peptide hydrogels were monitored via oscillatory frequency sweeps. The hydrogels were prepared using 1.9 wt% (19 mg $mL^{-1}$) of **P1** and of **P2** in the presence of 0.5 equiv. of $Zn(OAc)_2$. The samples were formed into silicon molds (Fig. S9), yielding similar transparent hydrogel discs with a 5 mm diameter. Three replicates of each hydrogel were prepared to ensure measurement accuracy. Viscoelasticity measurements were performed via frequency-sweep. The frequency sweep covered a spectrum of angular frequencies spanning from 0.1 to 100 rad $s^{-1}$, while maintaining a constant strain at 0.1%. Mechanical stiffness was assessed by plotting the elastic modulus, G′, against angular frequency, ω. Shear recovery analysis was carried out with sequential strain steps of 0.05% for 180 s, 100% for 180 s, and 0.05% for 600 s, repeated consecutively three times. These incremental steps facilitated the disruption of the hydrogel, inducing liquefaction, and enabled the monitoring of G′ and G″ recovery dynamics.

## 2.7 Scanning electron microscopy

Prior to the SEM measurements, all samples were shock-frozen in liquid nitrogen and lyophilized overnight using a Beta 2-8 LCSplus – Martin Christ lyophilizer. The morphology of the freeze-dried samples was visualized via a Zeiss Supra

https://doi.org/10.26434/chemrxiv-2024-00pc3 **ORCID:** https://orcid.org/0000-0002-6328-1896 Content not peer-reviewed by ChemRxiv. **License:** CC BY 4.0

55 VP microscope (Faculty Center for Nano Structure Research) with an accelerating voltage between 3 and 5 kV. The samples were carefully fixed onto carbon tape at the top of the aluminum specimen containers and placed on the specimen holder. Subsequently, they were sputter-coated with gold to a thickness of ~ 3 nm (Leica EM SCD050) and positioned at the specimen stage of the SEM. Measurements were performed at a magnification range of 40x to 2000x, using a Secondary Electrons detector.

### 2.8 Transmission electron microscopy

Prior to transmission electron microscopy (TEM) measurements, samples were suspended in water and drop-casted onto 200-mesh copper grids coated with carbon film. TEM was measured at the Electron Microscopy Facility at IST (Austria) using a Phillips Tecnai 12 (120kV) TEM equipped with a CMOS TVIPS TemCam-F216 camera. The resulting pictures were processed with Gatan Micrograph software and analyzed with TVIPS EM Measure beta 0.85.

## 3. Results and Discussion

### 3.1 Synthesis, peptide design and hydrogelation of Zn-responsive hydrogels

Amphiphilic peptides have been extensively investigated over the years for their role in self-assembly.[9, 45-47] Therefore, an amphiphilic sequence of amino acids was selected, consisting of one lipophilic (Leu, Ile, Val) and one hydrophilic (Lys, His) end. Two short amphiphilic peptides, Ac-LIVKHH-$NH_2$ (**P1**) and Fmoc-LIVKHH-$NH_2$ (**P2**), were designed based on their binding affinity to Zn(II) via their two histidine moieties. These histidine moieties can be deprotonated under physiological conditions, yielding imidazoles capable of coordinating to divalent zinc.[48, 49] Each peptide coordinates to two of the four sites available to the typically tetrahedral coordinated Zn(II), leading to a metal-peptide crosslinking node.[24, 50-52] (Fig. 1) Furthermore, *N*-terminus modification on one of the peptides is expected to exert a greater influence on hydrogel formation, particularly due to the presence of the Fmoc group in comparison with its acetylated analogue. The Fmoc group, known for its π-π stacking effects, facilitates the formation of stiffer hydrogels.[18]

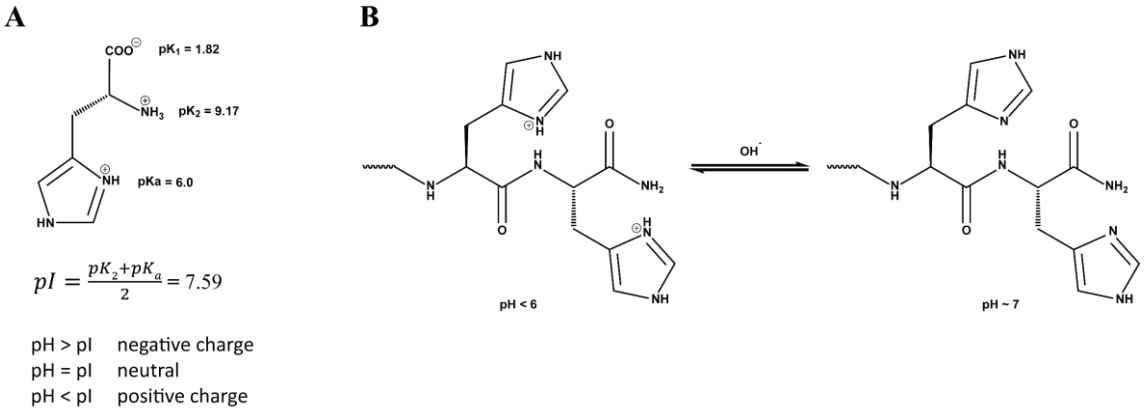


**Fig 1** (A) Histidine protonation, and (B) protonation or deprotonation of histidine moieties at different pH values of peptide solution.

The minimum gelation concentration was determined through dissolution of **P1** and **P2** in Milli-Q water at physiological conditions at different peptide concentrations. For **P1**, this was found to be 2 wt% (20 mg $mL^{-1}$), while **P2** displayed a minimum gelation concentration of 0.3 wt% (3 mg $mL^{-1}$). To test if the peptides indeed show stimuli responsiveness to Zn(II) ions, $Zn(OAc)_2$ was added to a peptide solution and the pH was readjusted to pH ~ 7. While a solution of **P2** in Milli-Q water takes about 5 minutes to form a hydrogel, the observed gelation time can be reduced to seconds in the presence of 0.5 equiv. $Zn(OAc)_2$, clearly demonstrating the influence of Zn(II) ions on the gelation behavior of **P2**.

Stiffer hydrogels, formed via higher peptide concentrations, required a shorter gelation period i.e., 2 wt% (20 mg $mL^{-1}$) of **P2** took only a few seconds for gelation, compared to 1 h for 0.3 wt% (3 mg $mL^{-1}$) (Fig. 2). The gels formed in MilliQ are transparent; however, when the concentration of metal exceeds 3 equiv. of the peptide, precipitation occurs. The gels formed in PBS are opaque. At peptide concentrations which are sufficiently high for hydrogel formation, the resulting hydrogels containing Zn(II) are stiffer than those without. The mechanical properties of the Zn-containing hydrogels differ when they are in buffer versus in Milli-Q water. The difference in their behavior was quantified and further assessed via oscillatory rheology (section 3.3).

https://doi.org/10.26434/chemrxiv-2024-00pc3 **ORCID:** https://orcid.org/0000-0002-6328-1896 Content not peer-reviewed by ChemRxiv. **License:** CC BY 4.0

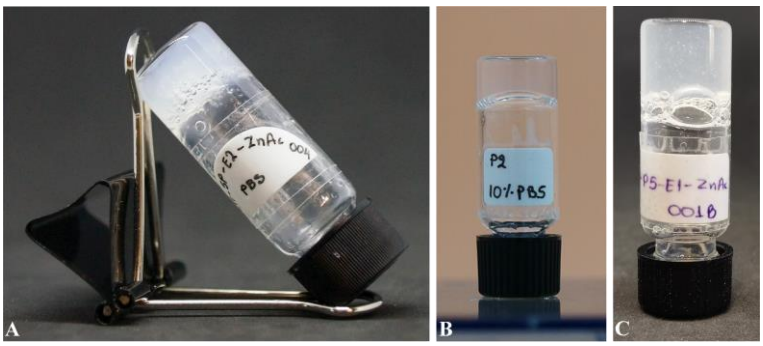


**Fig 2** Water based hydrogels of (A) **P2** at 1.9 wt% (19 mg $mL^{-1}$) in presence of 1 equiv. of Zn(II) in 10% PBS; (B) **P2** at 1.9 wt% (19 mg $mL^{-1}$) in 10% PBS; (C) **P2** in presence of 0.5 equiv. of Zn(II) in aqueous solution. [inversion test was used as an initial indication of gel formation, while gelation was verified via rheology measurements]

## 3.2 Structural conformation of stimuli-responsive hydrogels and microstructure

**P1** and **P2** each contain two histidines (Fig. 1B), which are positively charged below pH 6 (His(imidazole) $pK_a$ = 6.0). Under these conditions, the resulting electrostatic repulsion of peptides prevents self-assembly. Conversely, above pH 6, the deprotonation of the histidine moieties removes the electrostatic repulsion and facilitates Zn(II) binding, leading to rapid self-assembly and hydrogel formation (Fig. 3).[53]

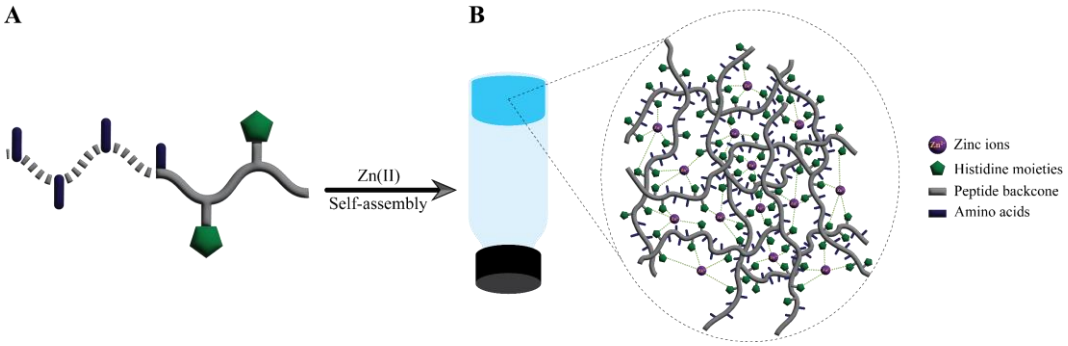


**Fig 3** (A) Part of peptide monomer, and (B) schematic of hydrogel formation in presence of Zn(II) that acts as polymerization agent favoring His-Zn-His coordination.

The secondary conformation of the peptides in the samples in presence and absence of Zn(II) was analysed by circular dichroism. In the absence of Zn(II), both **P1** (Fig. 4A) and **P2** (Fig. 4D) display a random coil conformation (negative peak between 190 and 200 nm) at low concentrations (0.5 mM, 4.86 mg $mL^{-1}$). As the concentration is increased, these conformations change, with **P1** transitioning to an α-helix conformation at 50 mM, evidenced by the replacement of the negative peak at 197 nm by two at 207 nm and 225 nm, whereas at 30 mM **P2** gives a strong positive peak at 199 nm, with no negative peaks at longer wavelength, indicating a conformation related to that of a β-sheet. In the presence of 0.5 equivalents of $Zn(OAc)_2$ (Fig. 4B and E), increasing the peptide concentration had little effect on the conformations of either of the peptides, with both giving CD signals consistent with random coil, as well as displaying some other small peaks which are not straightforward to assign. This suggests that the coordination crosslinks restrict the conformational space of the peptide and take precedence over prior conformational tendencies. In a 10% MES buffer and in the presence of Zn(II) (Fig. 4C and F), both peptides gave a classical random coil CD signal which increased in intensity as concentration was raised. In general, the presence of Zn(II) leads to Zn-imidazole coordination, which stabilizes the random coil structure, and may hinder the formation of a well-defined secondary structure. Thus, both peptides appear to have a relatively disordered, but flexible structure.

https://doi.org/10.26434/chemrxiv-2024-00pc3 **ORCID:** https://orcid.org/0000-0002-6328-1896 Content not peer-reviewed by ChemRxiv. **License:** CC BY 4.0

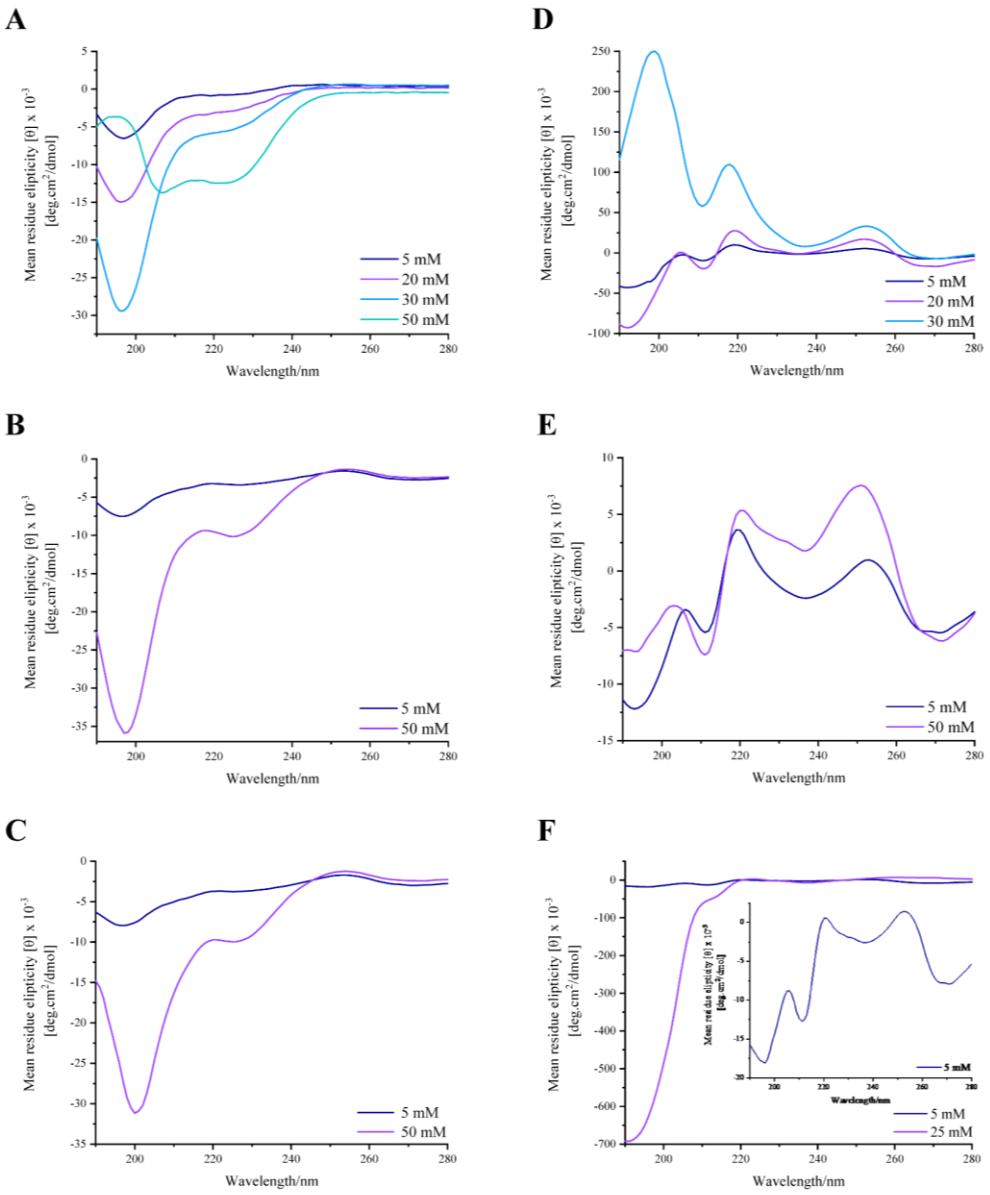


**Fig. 4** Circular dichroism (CD) scans of increasing concentration of **P1** (left column) and **P2** (right column) were conducted to monitor the changes in the secondary structure of peptides under various conditions. In graph A (**P1**) & graph D (**P2**), the scans were performed in aqueous solution at pH 7, showing a change in their structural conformation from random coil to α-helix and to β-sheet, respectively. In graph B (**P1**) and graph E (**P2**), the scans were conducted in an aqueous solution at pH 7 with 0.5 equiv. of $Zn(OAc)_2$, while in graph C (**P1**) and graph F (**P2**) additional scans were performed in a 10% MES buffer solution with 0.5 equiv. of $Zn(OAc)_2$. The peaks at 218 nm and 254 nm of D, E and F can be attributed to the Fmoc group.

The supramolecular architecture of the hydrogels was assessed further via scanning electron microscopy (SEM) and transmission electron microscopy (TEM). For SEM measurements, both **P1** and **P2** metallo-hydrogels were freeze-dried prior to the SEM measurements. The variations in the hydrogels' microstructure morphology can be observed in Fig. 5. All exhibit a flaky microporous structure. Similar structures have been reported in cases of metal-bearing hydrogels formed with coinage metal salts.[11, 54] The **P2** metallo-hydrogels in 10% PBS consistently demonstrate flaky formations throughout the sample (Fig. 5A&C), while the aqueous analogues demonstrate lamellae formations (Fig. 5C and D). Interestingly, in aqueous solution and at lower peptide concentration, P2 displayed fibrous networks in certain parts along the sample e.g., Fig. 5B. **P1** metallo-hydrogels exhibit lamellae formation in aqueous media.

TEM investigations further revealed that in absence of Zn(II), a fibrous network of long and flexible fibers is formed (Fig. 6A). However, the hydrogels containing 0.5 equiv. of Zn(II) tend to form a fibrous network of stacked and more straight nanofibers, whereby higher peptide concentrations result in shorter fibers, as shown in Fig. 6B and C, respectively.

https://doi.org/10.26434/chemrxiv-2024-00pc3 **ORCID:** https://orcid.org/0000-0002-6328-1896 Content not peer-reviewed by ChemRxiv. **License:** CC BY 4.0

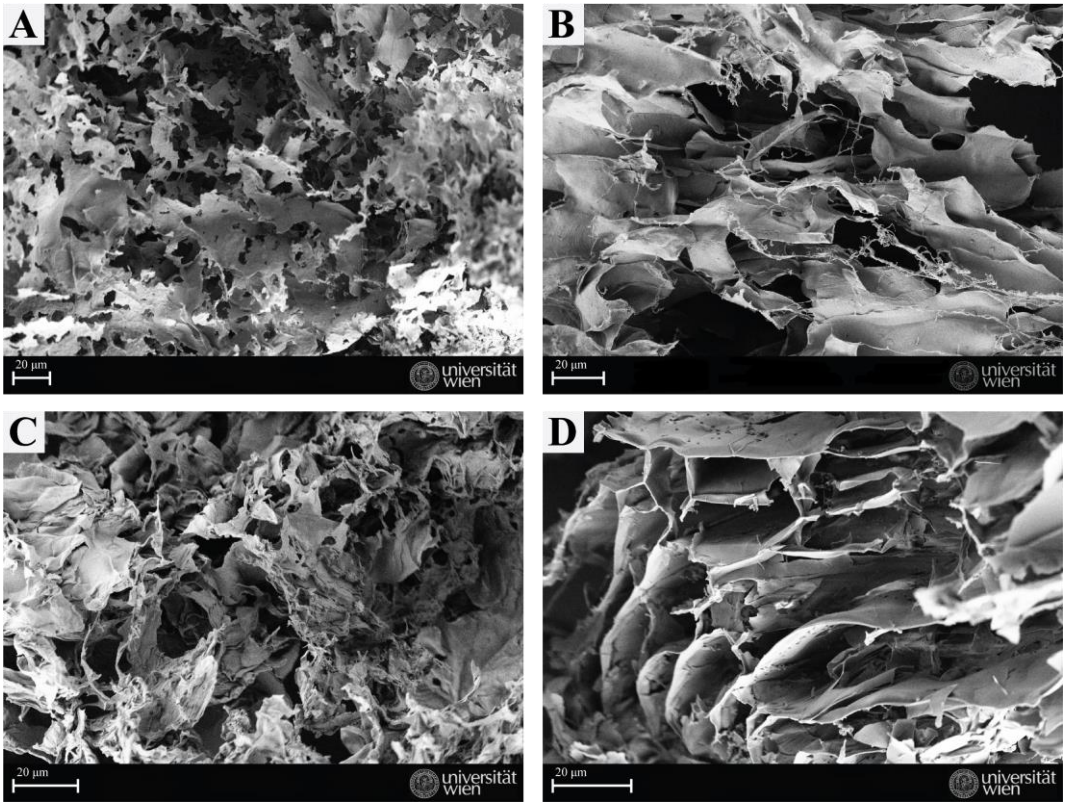


**Fig 5** SEM micrographs depicting the freeze-dried peptide hydrogels containing 0.5 equiv. of $Zn(OAc)_2$ formed with (A) 1.9 wt% (19 mg $mL^{-1}$) **P2** in 10% PBS buffer; (B) 0.3 wt% (3.4 mg·$mL^{-1}$) **P2** in MilliQ water; (C) 1.9 wt% (19 mg $mL^{-1}$) **P2** in 10% PBS buffer, and (D) 0.6 wt% (5.53 mg·$mL^{-1}$) **P1** in MilliQ water.

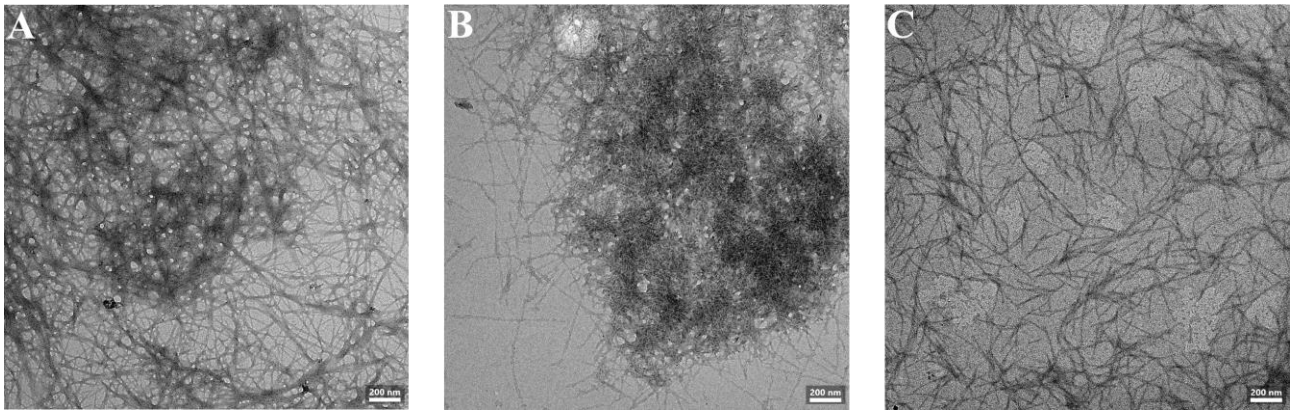


**Fig 6** TEM micrographs depicting peptide hydrogels containing (A) 0.2 wt% (2.66 mg $mL^{-1}$) **P2** in MilliQ water, pH adjusted to ~7 with 750 mM NaOH; (B) 0.5 equiv. of $Zn(OAc)_2$ formed with 0.2 wt% (2.66 mg $mL^{-1}$) **P2** in MilliQ water, pH adjusted to ~7 with 750 mM NaOH, and (C) 0.5 equiv. of Zn(OAc)2 formed with 1.9 wt% (19 mg $mL^{-1}$) **P2** in MilliQ water.

## 3.3 Assessment of viscoelastic properties of self-assembled peptide hydrogels

### 3.3.1 Rheology experiments

Mechanical stiffness and viscoelastic character of the peptide hydrogels were evaluated through oscillatory rheology experiments. Hydrogels were prepared at a consistent peptide concentration of 1.9 wt% (19 mg $mL^{-1}$) and pH ~7-7.4. A series of experiments were conducted to quantify the differences in hydrogel behavior between aqueous and 10% phosphate-buffered saline (PBS) solutions with and without Zn(II). The peptide concentration was carefully selected to ensure hydrogel formation in both cases.

Storage (G′) and loss (G″) moduli for all samples were quantified through an oscillatory rheology frequency sweep. Both peptides exhibit enhanced viscoelastic properties in 10% PBS in the presence of Zn(II) when compared to the samples without Zn(II). As mentioned above, we postulate that Zn(II) can act as a cross linker agent under physiological pH, facilitated by cross strand interactions (His-Zn-His) with the peptide, leading to improved mechanical properties of

https://doi.org/10.26434/chemrxiv-2024-00pc3 **ORCID:** https://orcid.org/0000-0002-6328-1896 Content not peer-reviewed by ChemRxiv. **License:** CC BY 4.0

hydrogels. In the absence of Zn(II), G′ values are significantly lower (Table 1), consistent with the slower and more loose formation of hydrogels.

In general, **P1** shows a lower tendency towards gelation compared to **P2**, due to the lack of the Fmoc moiety, which is known to enhance gelation via π-π stacking.[18, 55] At peptide concentrations of 1.9 wt% (19 mg $mL^{-1}$) and pH ~7-7.4, only **P2** (but not **P1**) hydrogels could be formed for both MQ and PBS solutions. With 0.5 equiv. of Zn(II), **P1** hydrogels formed for MQ but not PBS solutions (Fig. 7A, Table 1). The presence of Zn(II) aids hydrogel formation via coordinative binding by the histidine moieties, but PBS may lower the effective Zn(II) concentration via phosphate binding, preventing hydrogel formation.

**P2** hydrogels show stiffer viscoelastic properties in MQ rather than PBS solutions in the absence of Zn(II) (Fig. S10 A and B, respectively). However, with 0.5 equiv. of Zn(II), the **P2** hydrogels in MQ have similar mechanical strength with those with absence of Zn(II), but demonstrate a slight increase in mechanical strength only when increasing the temperature from 25 to 37 °C (Fig. 7B, Table 1). **P2** hydrogels in 10% PBS though become significantly stiffer and show no loss of mechanical strength or stiffness when increasing the temperature from 25 to 37 °C, but rather a slight increase in G′ to 0.304 MPa values (Fig. 7C, Table 1). Furthermore, across all conditions, G′ values consistently exceeded G″ values, indicating the presence of viscoelastic properties characteristic of a gel. When compared to other reported self-assembling peptide hydrogels (2-6 amino acids), our metal crosslinked hydrogels (**P1** and **P2)** display increased viscoelastic properties by at least one order of magnitude, thus clearly demonstrating potential of peptide hydrogels utilizing metals as cross linker.[13, 20, 23, 24, 26, 37, 38, 40, 56-66] Additionally, the reported G′ values and thixotropy (section 3.3.2) are on the verge of suitable for injection hydrogels, as they exceed the reported limit for injectable biomaterials.[15, 67-69]

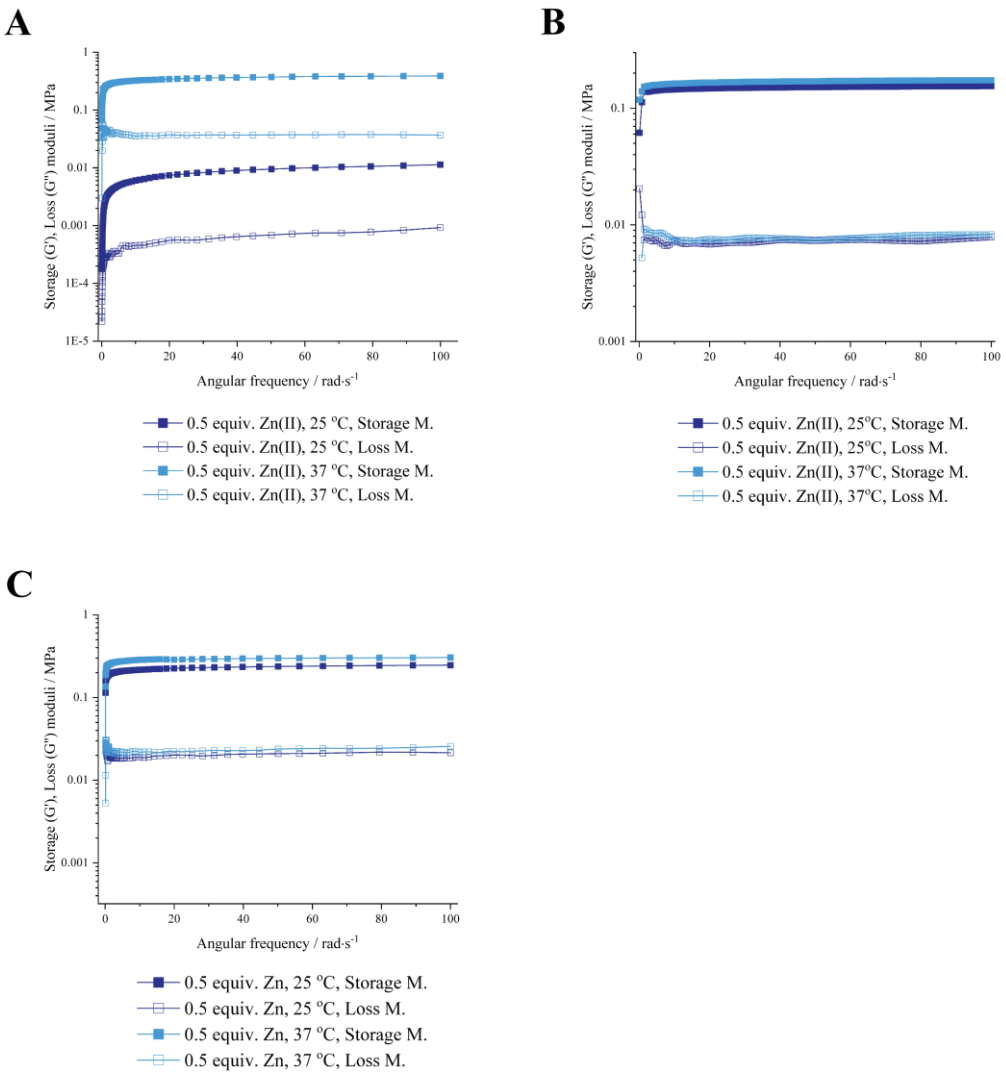


**Fig 7** Frequency sweep measurements were conducted for **P1** (A) and **P2** (B) to investigate the impact of $Zn^{2+}$ on the mechanical properties of hydrogels prepared in aqueous solution at both room temperature (25 °C) and physiological conditions (37 °C). Similarly, frequency sweep measurements were performed for **P2** (C) to assess the influence of $Zn^{2+}$ on the mechanical properties of hydrogels prepared in 10% PBS solution at room (25 °C) and physiological conditions (37 °C) (P1 can't form gel under these conditions).

https://doi.org/10.26434/chemrxiv-2024-00pc3 **ORCID:** https://orcid.org/0000-0002-6328-1896 Content not peer-reviewed by ChemRxiv. **License:** CC BY 4.0

**Table 1** Values of storage (G′) and loss (G″) modulus* of frequency sweep plots of **P1** and **P2** with or without $Zn^{2+}$.

| | | **P1** | | **P2** | |
|---|---|---|---|---|---|
| | Samples' characteristics | Storage M. (G′)/MPa | Loss M. (G″)/MPa | Storage M. (G′)/MPa | Loss M. (G″)/MPa |
| 25 °C | MilliQ, pH 7 | No gelation | No gelation | 0.150 | 0.019 |
| | 10% PBS | No gelation | No gelation | 0.004 | 0.0005 |
| | 0.5 equiv. Zn(II), MilliQ | 0.011 | 0.001 | 0.155 | 0.008 |
| | 0.5 equiv. Zn(II), 10% PBS | No gelation | No gelation | 0.246 | 0.022 |
| 37 °C | MilliQ, pH 7 | No gelation | No gelation | 0.152 | 0.018 |
| | 10% PBS | No gelation | No gelation | 0.011 | 0.0011 |
| | 0.5 equiv. Zn(II), MilliQ | 0.389 | 0.037 | 0.174 | 0.008 |
| | 0.5 equiv. Zn(II), 10% PBS | No gelation | No gelation | 0.304 | 0.026 |

*Highest recorded values are recorded from each plot

To put the observed values into the context of other biopolymer-based hydrogels, collagen was chosen as reference compound.[70-72] Both peptides outperform their collagen analogues, as illustrated in frequency sweep graphs and the above table (Fig. 8, Table 1 and 2), while buffer-based hydrogels exhibit enhanced viscoelastic properties compared with their aqueous analogues. The comparison between **P1** and **P2** with collagen demonstrates sufficient elasticity to endure the applied stress and strain as in bioengineering applications.[26, 73, 74]

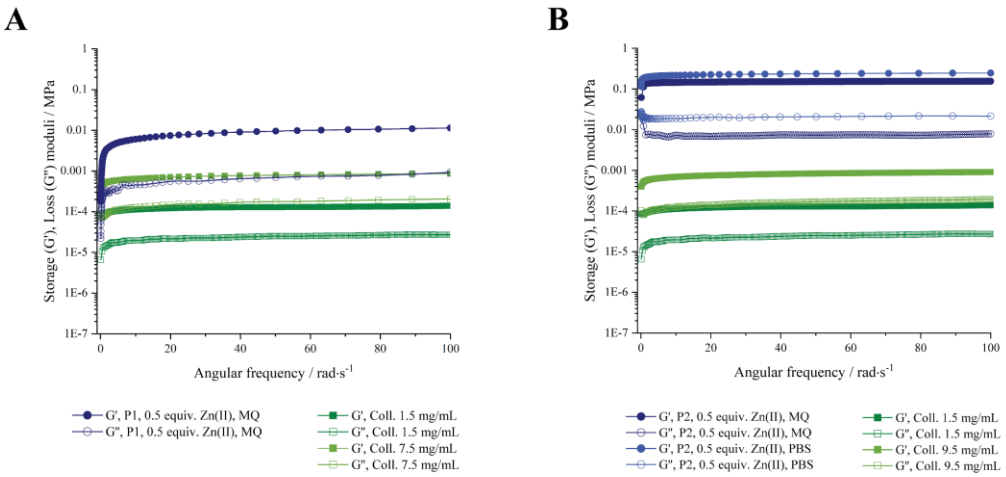


**Fig 8** Frequency sweep measurements were conducted for **P1** (A) and **P2** (B) hydrogels to compare the mechanical properties of **P1** and **P2** and their corresponding collagen analogues.

**Table 2** Values of storage (G′) and loss (G″) modulus* of frequency sweep plots of varying concentrations of collagen.

| | | **Collagen** | |
|---|---|---|---|
| | Samples' characteristics | Storage M. (G′)/MPa | Loss M. (G″)/MPa |
| 25 °C | | | |
| | Collagen 0.8 wt% (7.5 mg $mL^{-1}$) | 0.00086 | 0.00021 |
| | Collagen 1 wt% (9.5 mg $mL^{-1}$) | 0.00090 | 0.00020 |
| | Collagen 0.2 wt% (1.5 mg $mL^{-1}$) | 0.00014 | 0.000027 |

*Highest recorded values are recorded from each plot

### 3.3.2 Thixotropy experiments

The thixotropic behavior of **P2** hydrogels was systematically evaluated through step-strain rheology experiments. The extent of thixotropy is intricately linked to both the duration of applied shear stress, and the magnitude of the shear rate.[75] Both metallo-hydrogels and non-metallo-hydrogels exhibit remarkable thixotropic properties based on observations of their rapid recovery to the gel-like state. Upon the stopping of the shear force, the storage modulus (G′) of the **P2** hydrogel swiftly increased by more than three orders of magnitude within a few seconds. The gel-sol transition, induced by application of shear force, almost instantaneously reverses in a rapid sol-gel transition, once the shear force is discontinued (Fig. 9). Interestingly, it can also be seen that the presence of Zn(II) enhances by an order of magnitude both the G′ and G″ moduli of the **P2** hydrogel, without compromising the thixotropic behavior. The remarkable thixotropic behavior and recovery capacity of our peptide hydrogels, underscores their promise as injectable carriers or candidates for 3D printing applications.[67, 76]

https://doi.org/10.26434/chemrxiv-2024-00pc3 **ORCID:** https://orcid.org/0000-0002-6328-1896 Content not peer-reviewed by ChemRxiv. **License:** CC BY 4.0

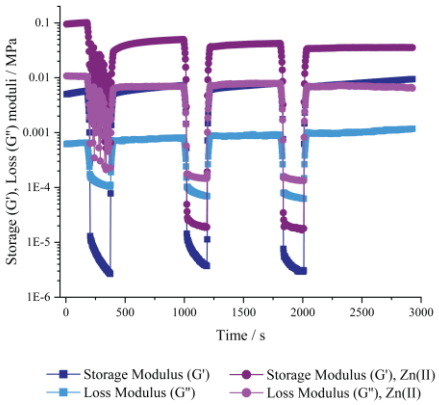


**Fig 9** Storage (G′) and Loss (G″) moduli were obtained from periodical oscillatory step experiments. **P2** hydrogels in a 10% PBS buffer solution were monitored with and without Zn(II) salt at room temperature (25 °C).

## 4. Conclusions

In summary, two novel amphiphilic peptides, namely Ac-LIVKHH-$NH_2$ (**P1**) and Fmoc-LIVKHH-$NH_2$ (**P2**), were designed, with the aim to bind to metals. Hereby, the incorporation of histidine residues facilitates the binding to Zn(II) ions. Zn(II) ions at physiological conditions are able to bind to deprotonated imidazole moieties via metal-peptide crosslinking. Thus, these peptides, demonstrated their binding affinity to Zn(II) ions with the adjacent histidine residues at pH ~ 7, and led to formation of metallo-hydrogels via coordination polymerization. The addition of Zn(II) resulted in rapid gelation, as observed due to the responsiveness of these hydrogels to chemical stimuli, such as pH change. Structural analyses, including circular dichroism spectroscopy, scanning electron microscopy, and transmission electron microscopy, provided valuable information about the supramolecular architecture and micro-/nanostructure of the hydrogels. The morphology of their micro- and nanostructure revealed a flexible fibrous network influenced with observable changes in the presences of Zn(II). Furthermore, at increasing peptide concentrations, while Zn(II) ions do not significantly impact the secondary conformation, they exhibit a stabilizing effect on the structure. Rheological characterization demonstrated the viscoelastic properties of the peptide hydrogels, along with their mechanical stiffness and thixotropic behavior. The incorporation of Zn(II) ions significantly enhanced the mechanical strength (and storage modulus) especially at physiological conditions. **P2** hydrogels showed thixotropic behavior in presence and absence of Zn(II) with rapid self-healing ability upon removal of shear force. To the best of our knowledge, the mechanical strength reported for our peptides, outperformed any other known (metallo)-hydrogels based on short peptides.[13, 22-24, 36-38, 40, 62, 77-81] As such, findings pave the way for the development of novel biomaterials with tailored properties for biomedical applications, including drug delivery, tissue engineering and wound healing/ management. Further, the thixotropic behavior of these peptides makes them ideal candidates for 3D printing or as injectable biomaterials for therapy.

## Acknowledgement

M. R. R. and J. C. thank the University of Vienna for financial support. This research was funded in whole or in part by the Austrian Science Fund (FWF) stand-alone grant no. P-34662 (M. R. R.) and by the ERC CoG no. 101002176 (J. C.). This research was supported by the Scientific Service Units of IST Austria through resources provided by the Electron Microscopy Facility.

## 5. References

1. Humana Press: **2018;** Vol. 1777.
2. M. Coste, E. Suárez-Picado and S. Ulrich, *Chemical Science* **2022,** *13* (4), 909-933.
3. P. D. Ross and S. Subramanian, *Biochemistry* **1981,** *20* (11), 3096-3102.
4. P. W. J. M. Frederix, G. G. Scott, Y. M. Abul-Haija, D. Kalafatovic, C. G. Pappas, N. Javid, N. T. Hunt, R. V. Ulijn and T. Tuttle, *Nature Chemistry* **2015,** *7* (1), 30-37.
5. A. Lakshmanan, S. Zhang and C. A. Hauser, *Trends Biotechnol.* **2012,** *30* (3), 155-65.
6. E. C. Wu, S. Zhang and C. A. E. Hauser, *Adv. Funct. Mater.* **2012,** *22* (3), 456-468.
7. O. S. Tiwari, R. Aizen, M. Meli, G. Colombo, L. J. W. Shimon, N. Tal and E. Gazit, *ACS Nano* **2023,** *17* (4), 3506-3517.
8. J. Li, X. Du, S. Hashim, A. Shy and B. Xu, *Journal of the American Chemical Society* **2017,** *139* (1), 71-74.
9. Y. Zhao, W. Yang, C. Chen, J. Wang, L. Zhang and H. Xu, *Current Opinion in Colloid & Interface Science* **2018,** *35*, 112-123.

https://doi.org/10.26434/chemrxiv-2024-00pc3 **ORCID:** https://orcid.org/0000-0002-6328-1896 Content not peer-reviewed by ChemRxiv. **License:** CC BY 4.0

10. J. Mayr, C. Saldias and D. Diaz Diaz, *Chem. Soc. Rev.* **2018,** *47* (4), 1484-1515.
11. X. Du, J. Zhou, J. Shi and B. Xu, *Chem. Rev.* **2015,** *115* (24), 13165-13307.
12. E. R. Draper and D. J. Adams, Design and Control of Hydrogels Formed by Self-assembly. In *Supramolecular Nanotechnology*, 2023; pp 619-639
13. W. Ji, C. Yuan, S. Zilberzwige-Tal, R. Xing, P. Chakraborty, K. Tao, S. Gilead, X. Yan and E. Gazit, *ACS Nano* **2019,** *13* (6), 7300-7309.
14. K. H. Chan, B. Xue, R. C. Robinson and C. A. E. Hauser, *Sci Rep* **2017,** *7* (1), 12897.
15. H. H. Susapto, D. Alhattab, S. Abdelrahman, Z. Khan, S. Alshehri, K. Kahin, R. Ge, M. Moretti, A. H. Emwas and C. A. E. Hauser, *Nano Lett.* **2021,** *21* (7), 2719-2729.
16. I. W. Hamley, *ACS Applied Bio Materials* **2023,** *6* (2), 384-409.
17. R. Orbach, I. Mironi-Harpaz, L. Adler-Abramovich, E. Mossou, E. P. Mitchell, V. T. Forsyth, E. Gazit and D. Seliktar, *Langmuir* **2012,** *28* (4), 2015-2022.
18. A. M. Smith, R. J. Williams, C. Tang, P. Coppo, R. F. Collins, M. L. Turner, A. Saiani and R. V. Ulijn, *Adv. Mater.* **2008,** *20* (1), 37-41.
19. W. F. Degrado and J. D. Lear, *Journal of the American Chemical Society* **1985,** *107* (25), 7684-7689.
20. K. H. Chan, W. H. Lee, M. Ni, Y. Loo and C. A. E. Hauser, *Sci Rep* **2018,** *8* (1), 17127.
21. Y. Zhang, H. Gu, Z. Yang and B. Xu, *Journal of the American Chemical Society* **2003,** *125* (45), 13680-13681.
22. N. Falcone and H. B. Kraatz, *Chemistry* **2018,** *24* (54), 14316-14328.
23. H. McEwen, E. Y. Du, J. P. Mata, P. Thordarson and A. D. Martin, *J Mater Chem B* **2017,** *5* (47), 9412-9417.
24. T. Shao, N. Falcone and H. B. Kraatz, *ACS Omega* **2020,** *5* (3), 1312-1317.
25. C. M. Micklitsch, P. J. Knerr, M. C. Branco, R. Nagarkar, D. J. Pochan and J. P. Schneider, *Angew. Chem. Int. Ed. Engl.* **2011,** *50* (7), 1577-9.
26. A. Mishra, Y. Loo, R. Deng, Y. J. Chuah, H. T. Hee, J. Y. Ying and C. A. E. Hauser, *Nano Today* **2011,** *6* (3), 232-239.
27. R. Zou, Q. Wang, J. Wu, J. Wu, C. Schmuck and H. Tian, *Chem. Soc. Rev.* **2015,** *44* (15), 5200-19.
28. P. Sharma, H. Kaur and S. Roy, *Biomacromolecules* **2019,** *20* (7), 2610-2624.
29. C. M. Rufo, Y. S. Moroz, O. V. Moroz, J. Stöhr, T. A. Smith, X. Hu, W. F. Degrado and I. V. Korendovych, *Nature Chemistry* **2014,** *6* (4), 303-309.
30. P. Bonaventura, G. Benedetti, F. Albarede and P. Miossec, *Autoimmun Rev* **2015,** *14* (4), 277-85.
31. C. Xu, Y. Cai, C. Ren, J. Gao and J. Hao, *Scientific Reports* **2015,** *5* (1), 7753.
32. M. Kurbasic, E. Parisi, A. M. Garcia and S. Marchesan, *Curr. Top. Med. Chem.* **2020,** *20* (14), 1300-1309.
33. T. Guan, J. Li, C. Chen and Y. Liu, *Advanced Science* **2022,** *9* (10), 2104165.
34. W. Y. Seow, G. Salgado, E. B. Lane and C. A. Hauser, *Sci Rep* **2016,** *6*, 32670.
35. I. Tengrup, J. Ahonen and B. Zederfeldt, *Surg Gynecol Obstet* **1981,** *152* (3), 323-6.
36. S. Basak, J. Nanda and A. Banerjee, *Chem Commun (Camb)* **2014,** *50* (18), 2356-9.
37. S. Basak, I. Singh and H.-B. Kraatz, *ChemistrySelect* **2017,** *2* (1), 451-457.
38. G. Li, M. Liu, C. Song and Z. Yuan, *Appl. Surf. Sci.* **2019,** *493*, 94-104.
39. V. Castelletto, I. W. Hamley, M. D. Segarra-Maset, C. B. Gumbau, J. F. Miravet, B. Escuder, J. Seitsonen and J. Ruokolainen, *Biomacromolecules* **2014,** *15* (2), 591-598.
40. A. Mishra, K.-H. Chan, M. R. Reithofer and C. A. E. Hauser, *RSC Advances* **2013,** *3* (25), 9985-9993.
41. E. Kaiser, R. L. Colescott, C. D. Bossinger and P. I. Cook, *Anal. Biochem.* **1970,** *34* (2), 595-598.
42. A. B. Inc., MES (0.5 M, pH 6) Preparation and Recipe. 2024;
43. I. Coin, M. Beyermann and M. Bienert, *Nat Protoc* **2007,** *2* (12), 3247-56.
44. S. I. Kirin, F. Noor and N. Metzler-nolte, *J. Chem. Educ.* **2007,** *84* (1), 108-111.
45. H. Qi, K. Qi, J. Li, C. He, M. Liao, X. Hu, Y. Zhao, Y. Ke, C. Zhang, J. Zhang, J. Wang, J. R. Lu and H. Xu, *Nano Research* **2023,** *16* (10), 12230-12237.
46. W. Ahn, J.-H. Lee, S. R. Kim, J. Lee and E. J. Lee, *Journal of Materials Chemistry B* **2021,** *9* (8), 1919-1940.
47. M. P. Hendricks, K. Sato, L. C. Palmer and S. I. Stupp, *Acc. Chem. Res.* **2017,** *50* (10), 2440-2448.
48. L. Zhou, S. Li, Y. Su, X. Yi, A. Zheng and F. Deng, *The Journal of Physical Chemistry B* **2013,** *117* (30), 8954-8965.
49. R. J. Sundberg and R. B. Martin, *Chem. Rev.* **1974,** *74* (4), 471-517.
50. S. Basak, I. Singh, A. Ferranco, J. Syed and H.-B. Kraatz, *Angew. Chem. Int. Ed.* **2017,** *56* (43), 13288-13292.
51. I. Sóvágó, K. Várnagy, N. Lihi and Á. Grenács, *Coord. Chem. Rev.* **2016,** *327-328*, 43-54.
52. D. W. Christianson and C. A. Fierke, *Acc. Chem. Res.* **1996,** *29* (7), 331-339.
53. M. Hesser, L. Thursch, T. Lewis, D. Diguiseppi, N. J. Alvarez and R. Schweitzer-Stenner, *Soft Matter* **2020,** *16* (17), 4110-4114.
54. I. Odriozola, P. Casuso, I. Loinaz, G. Cabañero and H. J. Grande, *Organic & Biomolecular Chemistry* **2011,** *9* (14), 5059.
55. A. Mahler, M. Reches, M. Rechter, S. Cohen and E. Gazit, *Adv. Mater.* **2006,** *18* (11), 1365-1370.
56. A. Lakshmanan, D. W. Cheong, A. Accardo, E. Di Fabrizio, C. Riekel and C. A. Hauser, *Proc Natl Acad Sci U S A* **2013,** *110* (2), 519-24.
57. M. R. Reithofer, A. Lakshmanan, A. T. K. K. Ping, J. M. Chin and C. A. E. E. Hauser, *Biomaterials* **2014,** *35* (26), 7535-7542.

https://doi.org/10.26434/chemrxiv-2024-00pc3 **ORCID:** https://orcid.org/0000-0002-6328-1896 Content not peer-reviewed by ChemRxiv. **License:** CC BY 4.0

58. J. Smadbeck, K. H. Chan, G. A. Khoury, B. Xue, R. C. Robinson, C. A. Hauser and C. A. Floudas, *PLoS Comput Biol* **2014,** *10* (7), e1003718.
59. Y. Loo, A. Lakshmanan, M. Ni, L. L. Toh, S. Wang and C. A. Hauser, *Nano Lett.* **2015,** *15* (10), 6919-25.
60. S. Rauf, H. H. Susapto, K. Kahin, S. Alshehri, S. Abdelrahman, J. H. Lam, S. Asad, S. Jadhav, D. Sundaramurthi, X. Gao and C. A. E. Hauser, *Journal of Materials Chemistry B* **2021,** *9* (4), 1069-1081.
61. D. Bairagi, P. Ghosh, P. Roy and A. Banerjee, *ACS Applied Nano Materials* **2023,** *6* (4), 2299-2309.
62. M. Mohammed, R. D. Chakravarthy and H.-C. Lin, *Molecular Systems Design & Engineering* **2022,** *7* (10), 1336-1343.
63. J. Wang, X.-Y. Chen, Y. Zhao, Y. Yang, W. Wang, C. Wu, B. Yang, Z. Zhang, L. Zhang, Y. Liu, X. Du, W. Li, L. Qiu, P. Jiang, X.-Z. Mou and Y.-Q. Li, *ACS Nano* **2019,** *13* (10), 11686-11697.
64. D. M. Raymond, B. L. Abraham, T. Fujita, M. J. Watrous, E. S. Toriki, T. Takano and B. L. Nilsson, *ACS Applied Bio Materials* **2019,** *2* (5), 2116-2124.
65. Y. Guo, S. Wang, H. Du, X. Chen and H. Fei, *Biomacromolecules* **2019,** *20* (1), 558-565.
66. Y. Xia, B. Xue, M. Qin, Y. Cao, Y. Li and W. Wang, *Sci Rep* **2017,** *7* (1), 9691.
67. M. H. Chen, L. L. Wang, J. J. Chung, Y.-H. Kim, P. Atluri and J. A. Burdick, *ACS Biomaterials Science & Engineering* **2017,** *3* (12), 3146-3160.
68. A. Schwab, R. Levato, M. D'Este, S. Piluso, D. Eglin and J. Malda, *Chem. Rev.* **2020,** *120* (19), 11028-11055.
69. S. Rauf, H. H. Susapto, K. Kahin, S. Alshehri, S. Abdelrahman, J. H. Lam, S. Asad, S. Jadhav, D. Sundaramurthi, X. Gao and C. A. E. Hauser, *J Mater Chem B* **2021,** *9* (4), 1069-1081.
70. J. J. Rice, M. M. Martino, L. De Laporte, F. Tortelli, P. S. Briquez and J. A. Hubbell, *Advanced Healthcare Materials* **2013,** *2* (1), 57-71.
71. T. Luo and K. L. Kiick, *Eur. Polym. J.* **2013,** *49* (10), 2998-3009.
72. A. Gaspar-Pintiliescu, A.-M. Stanciuc and O. Craciunescu, *Int. J. Biol. Macromol.* **2019,** *138*, 854-865.
73. Y. Loo, Y. C. Wong, E. Z. Cai, C. H. Ang, A. Raju, A. Lakshmanan, A. G. Koh, H. J. Zhou, T. C. Lim, S. M. Moochhala and C. A. Hauser, *Biomaterials* **2014,** *35* (17), 4805-14.
74. S. Sharma, V. K. Rai, R. K. Narang and T. S. Markandeywar, *Life Sci.* **2022,** *290*, 120096.
75. H. Herrada-Manchón, M. A. Fernández and E. Aguilar, *Gels* **2023,** *9* (7), 517.
76. Z. Zhang, S. Zhou, X. Wang, R. Liang, X. Sheng, Y. Zhu, L. Huang, B. Zhou and M. Zhong, *Materials Today Communications* **2023,** *36*, 106425.
77. B. Pramanik, *Gels* **2022,** *8* (9), 569.
78. D. M. Raymond, B. L. Abraham, T. Fujita, M. J. Watrous, E. S. Toriki, T. Takano and B. L. Nilsson, *ACS Applied Bio Materials* **2019,** *2* (5), 2116-2124.
79. Y. M. Abul-Haija, G. G. Scott, J. K. Sahoo, T. Tuttle and R. V. Ulijn, *Chem Commun (Camb)* **2017,** *53* (69), 9562-9565.
80. J. Chen, T. Wang and M. Liu, *Inorganic Chemistry Frontiers* **2016,** *3* (12), 1559-1565.
81. J. Mei, X. Zhang, M. Zhu, J. Wang, L. Wang and L. Wang, *RSC Adv.* **2014,** *4* (3), 1193-1196.

https://doi.org/10.26434/chemrxiv-2024-00pc3 **ORCID:** https://orcid.org/0000-0002-6328-1896 Content not peer-reviewed by ChemRxiv. **License:** CC BY 4.0